Estimating the spin diffusion length and the spin Hall angle from spin pumping induced inverse spin Hall voltages

Kuntal Roy*

School of Electrical and Computer Engineering, Purdue University, West Lafayette, Indiana 47907, USA

(Received 12 June 2017; published 22 November 2017)

There exists considerable confusion in estimating the spin diffusion length of materials with high spin-orbit coupling from spin pumping experiments. For designing functional devices, it is important to determine the spin diffusion length with sufficient accuracy from experimental results. An inaccurate estimation of spin diffusion length also affects the estimation of other parameters (e.g., spin mixing conductance, spin Hall angle) concomitantly. The spin diffusion length for platinum (Pt) has been reported in the literature in a wide range of 0.5–14 nm, and in particular it is a constant value independent of Pt's thickness. Here, the key reasonings behind such a wide range of reported values of spin diffusion length have been identified comprehensively. In particular, it is shown here that a thickness-dependent conductivity and spin diffusion length is necessary to simultaneously match the experimental results of effective spin mixing conductance and inverse spin Hall voltage due to spin pumping. Such a thickness-dependent spin diffusion length is tantamount to the Elliott-Yafet spin relaxation mechanism, which bodes well for transitional metals. This conclusion is not altered even when there is significant interfacial spin memory loss. Furthermore, the variations in the estimated parameters are also studied, which is important for technological applications.

DOI: 10.1103/PhysRevB.96.174432

I. INTRODUCTION

In the spin pumping [1–6] mechanism, unlike charge pumping [7], a precessing magnet sustained by an externally applied alternating magnetic field [8] emits *pure* spins into surrounding conductors. According to Onsager's reciprocity [9], spin pumping is the reciprocal phenomenon [10] of spin momentum transfer [11]. Theoretical constructs [3,4] well support the experimental results on spin pumping [2]. If the adjacent normal-metal possesses high spin-orbit coupling [12,13] (e.g., platinum [14], tantalum [15], tungsten [16], CuIr [17], CuBi [18], CuPb [19], AuW [20]), a considerable amount of dc charge voltage can be generated, allowing the detection of spin current via the inverse spin Hall effect (ISHE) [14,21–26]. Therefore, the spin pumping mechanism gives us an alternative methodology to understand and estimate the relevant parameters in the system. Such understandings can benefit the device design using SHE [27], which has potential for building future spintronic devices, along with other promising emerging devices [28].

From the spin pumping experiments there are three parameters to quantify: spin mixing conductance ($g^{\uparrow\downarrow}$) at the ferromagnet–normal-metal (FM-NM) interface [29,30], spin diffusion length (λ), and spin Hall angle (θ_{SH}) of the SHE layer acting as the NM layer. There are also the interface resistance and the spin flip parameter to identify when there is significant interfacial spin memory loss [31–34]. Experimentally, we get two quantities: effective spin mixing conductance ($g_{\rm eff}^{\uparrow\downarrow}$) of the whole structure from damping enhancement, and the induced inverse spin Hall voltage ($V_{\rm ISHE}$) due to the inverse spin Hall effect. There is controversy [35–62] in determining λ, which is reported in the wide range 0.5–14 nm. Such a wide range creates a massive issue in designing and predicting device functionality. We study the underlying theoretical constructs and address such an open issue. In particular, experimental results for permalloy (Py)/platinum (Pt) bilayers in Ref. [57] show that $g_{\rm eff}^{\uparrow\downarrow}$ and a quantity dependent on $V_{\rm ISHE}$ saturate at different thicknesses of the SHE layer ($\lambda \sim 1.5$ and 8.3 nm, respectively). However, Ref. [37] estimated a considerably different λ of 1.2 nm from experimental results of $V_{\rm ISHE}$, but the λ is fixed independent of the thickness of the Pt layer, according to the usual perception [40]. Also, Ref. [54] determines a λ of 7.3 nm from $V_{\rm ISHE}$, and Ref. [62] determines a λ of 0.8 nm from $g_{\rm eff}^{\uparrow\downarrow}$ recently for Py/Pt bilayers.

Here we analyze the key issues behind such major disagreements of the estimated values of the λ and its dependence of the SHE layer thickness. In room-temperature measurements, the issues are as follows: (i) The conductivities of the different samples used in different experiments are different. A higher conductivity σ would lead to a higher λ concomitantly ($\lambda \propto \sigma$), due to the Elliott-Yafet spin relaxation mechanism [63], which is relevant for transition metals [31,59,64,65]. (ii) With the Elliott-Yafet spin relaxation mechanism, λ is dependent on thickness since conductivity varies with the thickness of the sample (there is an interface contribution as well) [47]. The Dyakonov-Perel spin relaxation mechanism [66] corresponds to a constant λ, which is usually used but is not the relevant spin relaxation mechanism for transitional metals. (iii) A correct (must be positive) and relevant bare $g^{\uparrow\downarrow}$ must be used. The $g^{\uparrow\downarrow}$ is not achievable directly from experiments, rather what is achieved is an effective conductance of the whole bilayer $g_{\rm eff}^{\uparrow\downarrow}$, which is thickness-dependent. Also, the so-called Schep correction [4,67,68] needs to be performed on the bare $g^{\uparrow\downarrow}$, which makes a large difference. It is shown here that the controversy discussed in Ref. [57], namely that two different constant values of spin diffusion lengths are required to explain the experimental results of $g_{\rm eff}^{\uparrow\downarrow}$ and a quantity dependent on $V_{\rm ISHE}$, can be solved by considering a thickness-dependent λ [65].

*Present address: Department of Electrical Engineering and Computer Science, Indian Institute of Science Education and Research Bhopal, Bhopal 462066, Madhya Pradesh, India; kuntal@iiserb.ac.in; kuntalroy@gmail.com

 ©2017 American Physical Society

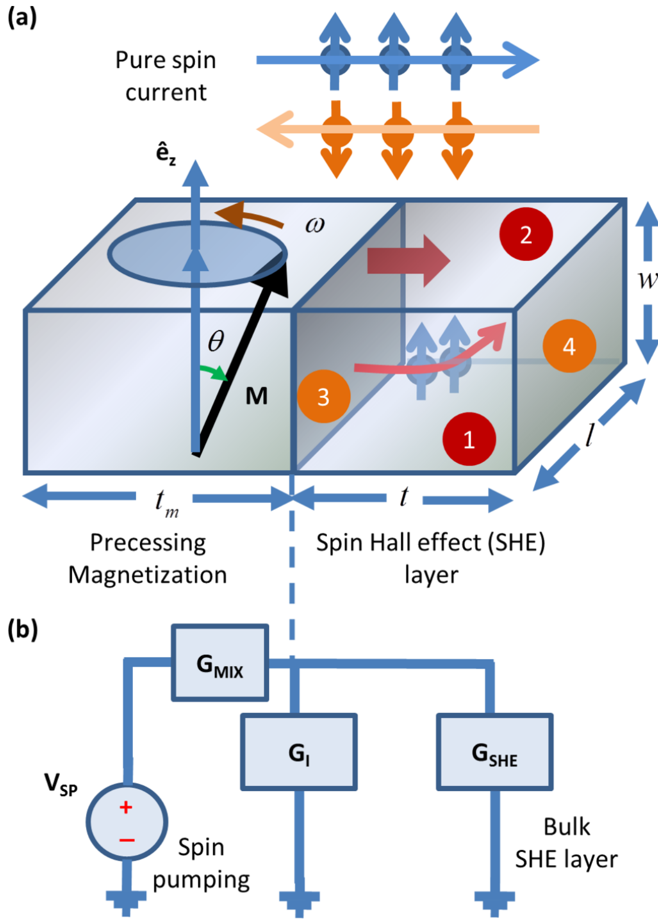

FIG. 1. (a) A precessing magnetization in a magnetic layer is pumping pure spin current into the adjacent normal metal (NM). If the normal metal has a high spin orbit coupling, a considerable amount of charge current can be produced due to the inverse spin Hall effect (ISHE). Spin potentials are developed at the surfaces marked by 3 and 4, while charge potentials are developed at the surfaces marked by 1 and 2. (b) In an equivalent spin circuit diagram, the voltage source V_{SP} acts as a spin battery, G_{MIX} is the interfacial spin mixing conductance between the magnetic layer and the SHE layer, G_I is the spin conductance representing the spin memory loss, and G_{SHE} is the spin conductance of the SHE layer, altered by the spin accumulation in the SHE layer in the presence of spin memory loss.

Since the variations in the estimated parameters pose limitations in designing technological applications, the variations in spin diffusion length and spin Hall angle are studied with respect to the variations in the interfacial spin mixing conductance and spin memory loss, which may be different due to the fabrication process and from sample to sample. It is found that the estimated parameters are quite sensitive to the interfacial conductances.

II. MODEL

Figure 1(a) shows a schematic diagram for spin pumping by a precessing magnetization into a SHE layer having a length l, width w, and thickness t. The thickness of the magnet is t_m. The corresponding spin circuit representation [65] containing the voltage source and conductances [69] is shown in Fig. 1(b). The voltage source V_{SP} acts as a spin battery [70], G_{MIX} is the interfacial bare spin mixing conductance between the magnetic layer and the SHE layer [29,30], G_I represents the spin conductance due to spin memory loss with parameter δ representing the spin flip probability $1-e^{-\delta}$ at the interface, and G_{SHE} is the spin conductance of the SHE layer, altered by the spin accumulation in the SHE layer in the presence of spin memory loss [31–34]. The conductances G_{MIX}, G_I, and G_{SHE} per unit area are defined as $G_{MIX}/lw = (2e^2/h)\, g^{\uparrow\downarrow}$, $G_I/lw = (\delta/R^*)\sinh(\delta) = (2e^2/h)\, g_I$, and $G_{SHE}/lw = (\sigma/\lambda)\cosh(\delta)\tanh(t/\lambda) = (2e^2/h)\, g_{SHE}$, where R^* is an effective interface resistance depending on the interface spin polarization [31–34], σ and λ are the conductivity and spin diffusion length of the SHE layer, respectively, and the conductances $g^{\uparrow\downarrow}$, g_I, and g_{SHE} are in units of m^{-2}. Note that R^* depends on σ [31]. The conductance g_{SHE} takes care of the backflow of the accumulated spins in the SHE layer [3,4].

The interfacial spin mixing conductance for FM-NM bilayers can be determined from first principles [71] as $\tilde{g}^{\uparrow\downarrow} = g_{Sh} - \sum r^{\uparrow}_{mn} r^{\downarrow *}_{mn}$ (where g_{Sh} is the so-called Sharvin conductance, i.e., the number of transport channels per unit area for one spin, and r^s_{mn} is the probability amplitude of reflection from channel n to channel m with the same spin s) [29,30], on which we have to perform the so-called Schep correction [4,67,68],

$$\frac{1}{g^{\uparrow\downarrow}} = \frac{1}{\tilde{g}^{\uparrow\downarrow}} - \frac{1}{2g_{Sh}}. \tag{1}$$

In general, the spin mixing conductance is a complex number; however, first-principles calculations and experimental results on the ferromagnetic resonance field shift show that the imaginary component is low for metallic interfaces [71], and therefore we mean only the real part here. According to Ref. [31], for Pt, $g^{\uparrow\downarrow}$ with spin orbit coupling is calculated *with* the Schep correction as $(h/e^2)1.07\times10^{15}$ m^{-2} and $g_{Sh} = (h/e^2)1\times10^{15}$ m^{-2}.

The effective spin mixing conductance of the spin circuit in Fig. 1(b) $G_{eff} = G_{MIX}||(G_I + G_{SHE}) = lw\,(2e^2/h)\, g^{\uparrow\downarrow}_{eff}$, where

$$g^{\uparrow\downarrow}_{eff} = \frac{g^{\uparrow\downarrow}(g_I + g_{SHE})}{g^{\uparrow\downarrow} + (g_I + g_{SHE})}. \tag{2}$$

The above equation can be written as

$$g^{\uparrow\downarrow} = \frac{g^{\uparrow\downarrow}_{eff}}{1 - g^{\uparrow\downarrow}_{eff}/(g_I + g_{SHE})}. \tag{3}$$

Since $g^{\uparrow\downarrow} > 0$, we can write

$$g^{\uparrow\downarrow}_{eff} < g_I + g_{SHE}, \tag{4}$$

which is true since the effective conductance $g^{\uparrow\downarrow}_{eff}$ of the circuit presented in Fig. 1(b) cannot be greater than the conductances due to spin memory loss at the interface and of the bulk SHE layer.

If the spin memory loss at the interface is negligible, i.e., $g_I \simeq 0$ [$\delta = 0$, $\sinh(\delta) = 0$, and $\cosh(\delta) = 1$], given an experimentally obtained value of $g^{\uparrow\downarrow}_{eff}$ and other parameters such as the thickness t and conductivity σ of the SHE layer, we can have a maximum critical possible value $\lambda_{crit} = (h/2e^2)(\sigma/g^{\uparrow\downarrow}_{eff})$. From Ref. [57], $g^{\uparrow\downarrow}_{eff} = 2.5\times10^{19}$ m^{-2}

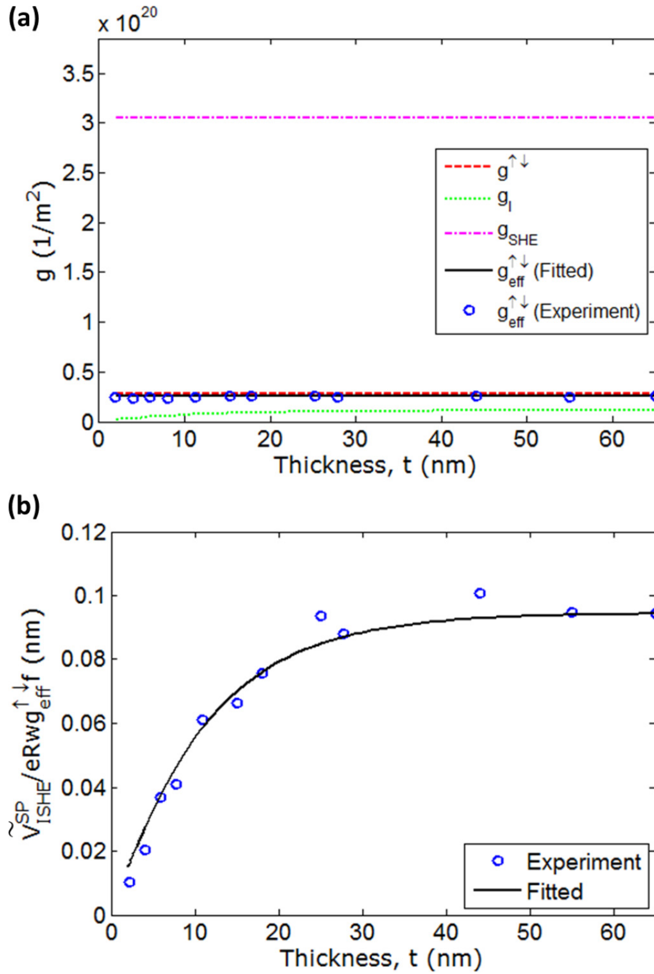

FIG. 2. Fitting the thickness t (2–65 nm) dependence of (a) effective spin-mixing conductance $g_{\text{eff}}^{\uparrow\downarrow}$ [Eq. (2)], and (b) a metric $\tilde{V}_{\text{ISHE}}^{\text{SP}}/eRwg_{\text{eff}}^{\uparrow\downarrow}f = \theta_{\text{SH}}\lambda\tanh(t/\lambda)$ [Eq. (5)]. Experimental data points are taken from Ref. [57], precisely for $f = 9$ GHz. In part (a), $g^{\uparrow\downarrow}$, g_I, and g_{SHE} are plotted as well.

at $t = 65$ nm, and $\sigma = 4.3 \times 10^6$ 1/Ω m, which gives $\lambda_{\text{crit}} = 2.19$ nm. In Refs. [58], $g_{\text{eff}}^{\uparrow\downarrow} = 2.1 \times 10^{19}$ m^{-2} at $t = 15$ nm, and $\sigma = 2.4 \times 10^6$ 1/Ω m, which gives $\lambda_{\text{crit}} = 1.475$ nm; however, λ is chosen as 10 nm therein, which is apparently inconsistent according to the underlying theoretical constructs as explained above [65]. It should be noted that with a significant spin memory loss (i.e., high g_I), Eq. (4) always tends to be satisfied.

From Eq. (2), note that $g_{\text{eff}}^{\uparrow\downarrow}$ is thickness-dependent due to the thickness dependence of g_{SHE} and the trend depends on how t/λ scales with lowering thickness, while $\lambda \propto \sigma$ according to the Elliott-Yafet spin relaxation mechanism. With t approaching zero, $g_{\text{eff}}^{\uparrow\downarrow}$ must go down to zero because both g_{SHE} and g_I go to zero (note $\delta = t_I/\lambda_I$, where t_I and λ_I are the interface thickness and interface spin diffusion length, respectively, goes toward zero, too). It is possible to measure experimentally both $g_{\text{eff}}^{\uparrow\downarrow}$ (from the enhancement of damping) and conductivity σ with thickness t. Then choosing a value of $\lambda_{\max}$ (at very high thickness $t \gg \lambda$) and (R^*,δ) representing interfacial spin memory loss, $g^{\uparrow\downarrow}$ can be calculated from Eq. (3). Using ($\lambda_{\max}$,$g^{\uparrow\downarrow}$), (R^*,δ), and the relation $\lambda(t) \propto \sigma(t)$, we can calculate $g_{\text{eff}}^{\uparrow\downarrow}(t)$ from Eq. (2). We can choose the $\lambda_{\max}$ and (R^*,δ) that give us the best fit with the experimental data and the corresponding $g^{\uparrow\downarrow}$ to characterize the experimental results of $g_{\text{eff}}^{\uparrow\downarrow}(t)$.

Note that the total effective spin-mixing conductance $g_{\text{eff}}^{\uparrow\downarrow}$ (that includes any possible spin memory loss), which can be determined experimentally from the enhancement of damping due to spin pumping in ferromagnetic resonance experiments [3,4], is the one that is important for the measurement of the inverse spin Hall voltage V_{ISHE} along the length of the SHE layer. Reference [57] defines a metric $\tilde{V}_{\text{ISHE}}^{\text{SP}}$ from the measurement of V_{ISHE} and uses the relation

$$\frac{\tilde{V}_{\text{ISHE}}^{\text{SP}}}{eRwg_{\text{eff}}^{\uparrow\downarrow}f} = \theta_{\text{SH}}\lambda\tanh\left(\frac{t}{2\lambda}\right), \quad (5)$$

where θ_{SH} is the spin Hall angle and R is the resistance of the bilayer, which is the inverse of $(\sigma t + \sigma_m t_m)\, w/l$ (σ_m is the conductivity of the magnetic layer). Note that such an expression is similar to the expression derived in Ref. [58]. The frequency-dependent elliptical precession factor P (Ref. [72]) used in Ref. [58] is included in the metric $\tilde{V}_{\text{ISHE}}^{\text{SP}}$ in Ref. [57] and attributed to the in-pane and out-of-plane precessing angles. Note that the metric defined by Eq. (5) is quite frequency-independent, as the ferromagnetic resonance measurement results show in Ref. [57] for 8 and 9 GHz. Also, note that the spin rectification voltage needs to be separated from the inverse spin Hall voltage V_{ISHE} [39,57,58].

III. RESULTS AND DISCUSSIONS

Figure 2 shows the fitting of the experimental results $g_{\text{eff}}^{\uparrow\downarrow}$ and $\tilde{V}_{\text{ISHE}}^{\text{SP}}/eRwg_{\text{eff}}^{\uparrow\downarrow}f$ from Ref. [57]. Equations (2) and (5) have been used to match the experimental results. The thickness t dependence of conductivity σ and spin diffusion length λ, which is plotted in Fig. 3, is utilized here to successfully match the experimental results of $g_{\text{eff}}^{\uparrow\downarrow}$ and $\tilde{V}_{\text{ISHE}}^{\text{SP}}/eRwg_{\text{eff}}^{\uparrow\downarrow}f$ *simultaneously*. Otherwise, according to Ref. [57], it would have taken two thickness-independent spin diffusion lengths (~1.5 and 8.3 nm) to match $g_{\text{eff}}^{\uparrow\downarrow}$ and $\tilde{V}_{\text{ISHE}}^{\text{SP}}/eRwg_{\text{eff}}^{\uparrow\downarrow}f$, respectively, which is unreasonable and is

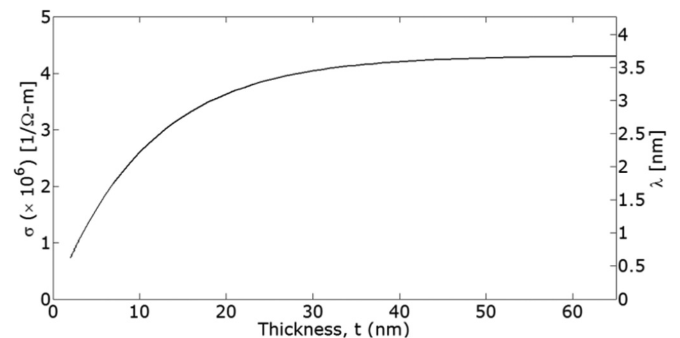

FIG. 3. Thickness t (2–65 nm) dependence of conductivity and spin diffusion length λ. Due to the Elliot-Yafet spin relaxation mechanism, $\lambda \propto \sigma$, and σ depends on the thickness t. The saturated value $\lambda_{\max}$ ($\sigma_{\max}$) = 3.67 nm (4.3 × 10^6 1/Ω m) and the lowest value of λ (σ) = 0.62 nm (0.73 × 10^6 1/Ω m) at $t = 2$ nm.

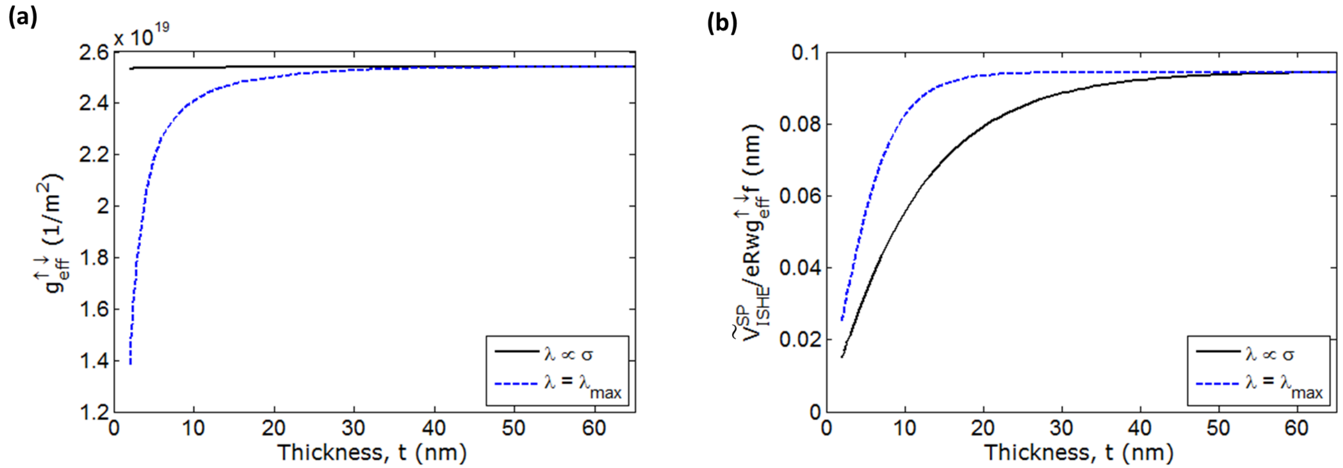

FIG. 4. Thickness t (2–65 nm) dependence of (a) effective spin-mixing conductance $g_{\rm eff}^{\uparrow\downarrow}$ [Eq. (2)], and (b) a metric $\tilde{V}_{\rm ISHE}^{\rm SP}/eRwg_{\rm eff}^{\uparrow\downarrow}f = \theta_{\rm SH}\lambda\tanh(t/\lambda)$ [Eq. (5)] for two cases: $\lambda \propto \sigma$ (Elliott-Yafet spin relaxation mechanism) and $\lambda = \lambda_{\rm max} = 3.67$ nm (Dyakonov-Perel spin relaxation mechanism).

deemed as a controversy therein. We get from Ref. [31] $g^{\uparrow\downarrow} = 2.76 \times 10^{19}$ m^{-2} and $g_I = 1.11 \times 10^{19}$ m^{-2} using $\delta = 3.7$ and $R^*/\delta = 23.6$ fΩ m^2 (i.e., $R^* = 87.3$ fΩ m^2) at $\sigma = 4.3 \times 10^6$ 1/Ω m. According to Ref. [57], $g_{\rm eff}^{\uparrow\downarrow} = 2.5 \times 10^{19}$ m^{-2} at $t = 65$ nm, and $\sigma = 4.3 \times 10^6$ 1/Ω m. Hence we determine $\lambda_{\rm max} = 3.67$ nm at the high thickness regime $t \gg \lambda$ using the following equation:

$$\lambda_{\rm max} = \frac{h}{2e^2}\frac{\sigma_{\rm max}\cosh(\delta)}{g^{\uparrow\downarrow}g_{\rm eff}^{\uparrow\downarrow}/(g^{\uparrow\downarrow} - g_{\rm eff}^{\uparrow\downarrow}) - g_I}. \quad (6)$$

Figure 3 shows the thickness t dependence of conductivity σ and spin diffusion length λ with $\lambda \propto \sigma$ signifying the Elliott-Yafet spin relaxation mechanism. Reference [57] specifies the experimental value of conductivity 4.3×10^6 1/Ω m, which is a relevant saturated bulk value of conductivity [38]. However, since Ref. [57] does not provide any thickness-dependent data of σ, the trend of conductivity with thickness is taken from the experimental data provided in Ref. [47] with a fitting of $\sigma = 4.3 \times 10^6 \times (1 - e^{-t/10.84\ \rm nm})$. A similar fitting model is used in Ref. [38]. As calculated earlier, the value of $\lambda_{\rm max}$ ($\sigma_{\rm max}$) = 3.67 nm (4.3×10^6 1/Ω m).

Figure 4 compares the results assuming the Dyakonov-Perel spin relaxation mechanism, with $\lambda = \lambda_{\rm max} = 3.67$ nm. The comparison shows pretty clearly that two different spin diffusion lengths (~1.5 and 8.3 nm) would have been necessary to match the parts (a) and (b), respectively, according to Ref. [57] along with the assumption that conductivity σ is independent of thickness. Therefore, the assumptions are inconsistent in different ways, and we do not assume that σ is constant with t in Fig. 4. As shown in Fig. 2, $\lambda \propto \sigma$ (signifying the Elliott-Yafet spin relaxation mechanism) gives the correct fit for both parts (a) and (b), *simultaneously*.

Figure 5(a) shows the $\lambda_{\rm max}$ (0.5–15 nm) dependence of the different conductances involved while keeping $g_{\rm eff}^{\uparrow\downarrow}$ constant, since this is directly obtained from experiments. For a certain

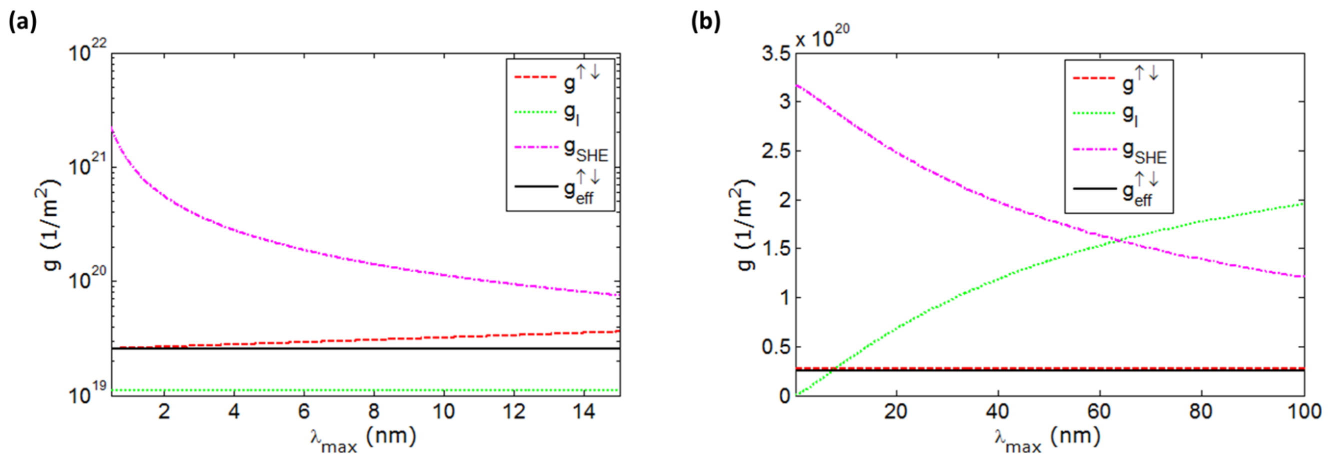

FIG. 5. (a) The $\lambda_{\rm max}$ (0.5–15 nm) dependence of $g^{\uparrow\downarrow}$ and $g_{\rm SHE}$ for a constant effective spin mixing conductance $g_{\rm eff}^{\uparrow\downarrow}$ and constant g_I representing the interfacial spin memory loss. $g^{\uparrow\downarrow}$ increases with increasing $\lambda_{\rm max}$ while $g_{\rm SHE}$ follows the opposite trend. (b) The $\lambda_{\rm max}$ dependence of g_I and $g_{\rm SHE}$ for constant values of $g_{\rm eff}^{\uparrow\downarrow}$ and $g^{\uparrow\downarrow}$. The spin flip parameter δ is varied from 0 to 6.07 while the interface resistance is kept constant at $R^* = 87.3$ fΩ m^2. Hence, the $\lambda_{\rm max}$ varies from 0.18 to 98 nm. g_I increases with increasing $\lambda_{\rm max}$ while $g_{\rm SHE}$ follows the opposite trend. The thickness t of the SHE layer for both cases is 65 nm.

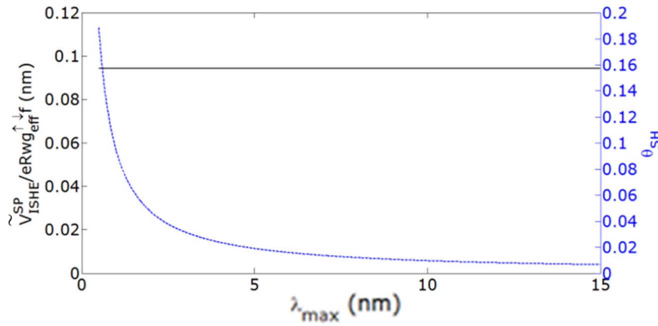

FIG. 6. The λ_{max} (0.5–15 nm) dependence of the spin Hall angle θ_{SH} while keeping the metric $\tilde{V}_{\mathrm{ISHE}}^{\mathrm{SP}}/eRwg_{\mathrm{eff}}^{\uparrow\downarrow}f=\theta_{\mathrm{SH}}\lambda\tanh(t/\lambda)$ [Eq. (5)] constant. The thickness t is assumed to be 65 nm. The θ_{SH} decreases with increasing λ_{max} keeping $\theta_{\mathrm{SH}}\lambda_{\mathrm{max}}$ constant.

value of $g_{\mathrm{eff}}^{\uparrow\downarrow}$, as λ_{max} increases, the spin conductance of the SHE layer g_{SHE} decreases, and therefore the interfacial spin mixing conductance $g^{\uparrow\downarrow}$ increases. (The conductance due to interfacial spin memory loss g_I is kept constant.) However, the change in $g^{\uparrow\downarrow}$ is less than 3% for the range of λ_{max} with reference to the nominal value of $g^{\uparrow\downarrow}=2.76\times10^{19}\ \mathrm{m}^{-2}$ at $\lambda_{\mathrm{max}}=3.67$ nm. Therefore, a slight variation in $g^{\uparrow\downarrow}$ can lead to a large variation in λ_{max}.

Figure 5(b) shows the trend of g_I and g_{SHE} with λ_{max} when the interface spin flip parameter δ varied between 0 and 6.07, and R^*, $g_{\mathrm{eff}}^{\uparrow\downarrow}$, and $g^{\uparrow\downarrow}$ are kept constant. The range of λ_{max} turns out to be 0.18 nm ($g_I=0$) through 98 nm ($g_I=1.94\times10^{20}\ \mathrm{m}^{-2}$). The g_{SHE} decreases (with the increase of both δ and λ_{max}) with increasing λ_{max} so that the sum g_I+g_{SHE} is constant at $3.168\times10^{20}\ \mathrm{m}^{-2}$. With a sufficient increase of δ, g_I starts to take over g_{SHE} at $\delta=5.9$ and $\lambda_{\mathrm{max}}=64.32$ nm. A further increase of δ makes g_I equal to $3.168\times10^{20}\ \mathrm{m}^{-2}$, the sum of g_I+g_{SHE} with g_{SHE} tending to zero, and such a maximum value δ_{max} can be calculated as 6.4919 by solving the following equation:

$$\delta_{\mathrm{max}}\sinh(\delta_{\mathrm{max}})=\frac{2e^2}{h}R^*\frac{g^{\uparrow\downarrow}g_{\mathrm{eff}}^{\uparrow\downarrow}}{g^{\uparrow\downarrow}-g_{\mathrm{eff}}^{\uparrow\downarrow}}. \tag{7}$$

Figure 6 shows that the spin Hall angle θ_{SH} decreases inversely proportional to λ_{max} for a certain value of the metric on the left-hand side of Eq. (5). Therefore, for a given λ_{max}, we get θ_{SH}. Hence, we can get the set (λ_{max},θ_{SH},$g^{\uparrow\downarrow}$) as (3.67 nm, 0.026, $2.76\times10^{19}\ \mathrm{m}^{-2}$) that we have used to match the experimental results as depicted in the Fig. 2. However, these two sets (7 nm, 0.014, $2.98\times10^{19}\ \mathrm{m}^{-2}$) and (0.50 nm, 0.19, $2.57\times10^{19}\ \mathrm{m}^{-2}$) would also match the experimental results in Fig. 2. It should be noted that the factor $t/\lambda(t)$ at $t=2$ nm for the aforementioned three sets is 3.04 [λ (2 nm) = 0.66 nm], 1.69 [λ (2 nm) = 1.18 nm], and 23.68 [λ (2 nm) = 0.08 nm], respectively, making the $\tanh(t/\lambda)$ term greater than 0.9. For all these calculations, $g_I=1.95\times10^{18}\ \mathrm{m}^{-2}$. Therefore, an understanding of any one parameter of the set (λ_{max},θ_{SH},$g^{\uparrow\downarrow}$) is required to get the complete set. We have utilized $g^{\uparrow\downarrow}$ from first-principles calculations [31], and we described in Sec. II that experimental data on thickness-dependent $g_{\mathrm{eff}}^{\uparrow\downarrow}$ (at the low-thickness regime where $g_{\mathrm{eff}}^{\uparrow\downarrow}$ varies) can provide us with an accurate set (λ_{max},$g^{\uparrow\downarrow}$,g_I). Also, it may be possible to know θ_{SH} from the spin-torque ferromagnetic resonance [73–75], or λ from other experiments [59,76,77].

IV. SUMMARY

To summarize, we have shown that a thickness-dependent spin diffusion length for platinum signifying the Elliott-Yafet spin relaxation mechanism is necessary to *simultaneously* match the experimental results of thickness-dependent effective spin mixing conductance and the inverse spin Hall voltage induced by spin pumping. A similar analysis can be applied to other SHE materials, e.g., palladium (Pd) [36,50,58,60,78], tantalum (Ta) [15,43,60,79–81], and tungsten (W) [16]. We note that there is some controversy in the literature regarding significant interfacial spin memory loss (a significant loss makes the spin diffusion length higher) [31,32,34,48,74,76,82–84]. However, as analyzed, the conclusion presented in this paper remains the same. The sample quality, i.e., conductivity, can apparently result in a large variation in spin diffusion length and spin Hall angle [85]. Note that the spin Hall angle discussed here is an effective one since the interface spin Hall effect can be different from its bulk counterpart in general [86,87]. We must also carefully consider the low-thickness regime (<2 nm) due to the magnetic proximity effect [88–92]. Since the estimated parameters are sensitive to the variation in interface conductances, variation-tolerant design principles may need to be employed for engineering applications. The comprehensive analysis performed here has immense consequences on device design and predicting correct device functionality for potential technological applications.

ACKNOWLEDGMENTS

This work was supported by FAME, one of six centers of STARnet, a Semiconductor Research Corporation program sponsored by MARCO and DARPA.

[1] R. H. Silsbee, A. Janossy, and P. Monod, Phys. Rev. B **19**, 4382 (1979).

[2] S. Mizukami, Y. Ando, and T. Miyazaki, J. Magn. Magn. Mater. **226**, 1640 (2001); Jpn. J. Appl. Phys. **40**, 580 (2001); Phys. Rev. B **66**, 104413 (2002); J. Magn. Magn. Mater. **239**, 42 (2002); B. Heinrich, K. B. Urquhart, A. S. Arrott, J. F. Cochran, K. Myrtle, and S. T. Purcell, Phys. Rev. Lett. **59**, 1756 (1987); R. Urban, G. Woltersdorf, and B. Heinrich, *ibid.* **87**, 217204 (2001); W. Platow, A. N. Anisimov, G. L. Dunifer, M. Farle, and K. Baberschke, Phys. Rev. B **58**, 5611 (1998).

[3] Y. Tserkovnyak, A. Brataas, and G. E. W. Bauer, Phys. Rev. Lett. **88**, 117601 (2002); Phys. Rev. B **66**, 224403 (2002).

[4] Y. Tserkovnyak, A. Brataas, G. E. W. Bauer, and B. I. Halperin, Rev. Mod. Phys. **77**, 1375 (2005).

[5] M. V. Costache, M. Sladkov, S. M. Watts, C. H. van der Wal, and B. J. van Wees, Phys. Rev. Lett. **97**, 216603 (2006).
[6] K. Ando, S. Takahashi, J. Ieda, H. Kurebayashi, T. Trypiniotis, C. H. W. Barnes, S. Maekawa, and E. Saitoh, Nat. Mater. **10**, 655 (2011).
[7] P. W. Brouwer, Phys. Rev. B **58**, R10135 (1998); M. Büttiker, H. Thomas, and A. Prêtre, Z. Phys. B **94**, 133 (1994).
[8] Y. Guan, W. E. Bailey, E. Vescovo, C.-C. Kao, and D. A. Arena, J. Magn. Magn. Mater. **312**, 374 (2007).
[9] L. Onsager, Phys. Rev. **37**, 405 (1931); **38**, 2265 (1931).
[10] A. Brataas, Y. Tserkovnyak, G. E. W. Bauer, and P. J. Kelly, Spin pumping and spin transfer, in *Spin Current*, edited by S. Maekawa, S. O. Valenzuela, E. Saitoh, and T. Kimura (Oxford University Press, Oxford, 2012), Vol. 17, pp. 87–135.
[11] J. C. Slonczewski, J. Magn. Magn. Mater. **159**, L1 (1996); L. Berger, Phys. Rev. B **54**, 9353 (1996); J. Z. Sun, *ibid.* **62**, 570 (2000); M. D. Stiles and A. Zangwill, *ibid.* **66**, 014407 (2002).
[12] T. Tanaka, H. Kontani, M. Naito, T. Naito, D. S. Hirashima, K. Yamada, and J. Inoue, Phys. Rev. B **77**, 165117 (2008).
[13] A. A. Abrikosov and L. P. Gor'kov, Sov. Phys. JETP **15**, 752 (1962).
[14] T. Kimura, Y. Otani, T. Sato, S. Takahashi, and S. Maekawa, Phys. Rev. Lett. **98**, 156601 (2007).
[15] L. Liu, C. F. Pai, Y. Li, H. W. Tseng, D. C. Ralph, and R. A. Buhrman, Science **336**, 555 (2012).
[16] C. F. Pai, L. Liu, Y. Li, H. W. Tseng, D. C. Ralph, and R. A. Buhrman, Appl. Phys. Lett. **101**, 122404 (2012).
[17] Y. Niimi, M. Morota, D. H. Wei, C. Deranlot, M. Basletic, A. Hamzic, A. Fert, and Y. Otani, Phys. Rev. Lett. **106**, 126601 (2011).
[18] Y. Niimi, Y. Kawanishi, D. H. Wei, C. Deranlot, H. X. Yang, M. Chshiev, T. Valet, A. Fert, and Y. Otani, Phys. Rev. Lett. **109**, 156602 (2012).
[19] Y. Niimi, H. Suzuki, Y. Kawanishi, Y. Omori, T. Valet, A. Fert, and Y. Otani, Phys. Rev. B **89**, 054401 (2014).
[20] P. Laczkowski, J. C. Rojas-Sánchez, W. Savero-Torres, H. Jaffrès, N. Reyren, C. Deranlot, L. Notin, C. Beigné, A. Marty, and J. P. Attané, Appl. Phys. Lett. **104**, 142403 (2014).
[21] A. Azevedo, L. H. Vilela-Leão, R. L. Rodríguez-Suárez, A. B. Oliveira, and S. M. Rezende, J. Appl. Phys. **97**, 10C715 (2005).
[22] X. Wang, G. E. W. Bauer, B. J. van Wees, A. Brataas, and Y. Tserkovnyak, Phys. Rev. Lett. **97**, 216602 (2006).
[23] E. Saitoh, M. Ueda, H. Miyajima, and G. Tatara, Appl. Phys. Lett. **88**, 182509 (2006).
[24] S. O. Valenzuela and M. Tinkham, Nature (London) **442**, 176 (2006).
[25] K. Ando, S. Takahashi, J. Ieda, Y. Kajiwara, H. Nakayama, T. Yoshino, K. Harii, Y. Fujikawa, M. Matsuo, and S. Maekawa, J. Appl. Phys. **109**, 103913 (2011).
[26] C. Hahn, G. de Loubens, M. Viret, O. Klein, V. V. Naletov, and J. Ben Youssef, Phys. Rev. Lett. **111**, 217204 (2013).
[27] K. Roy, J. Phys. D **47**, 422001 (2014).
[28] K. Roy, SPIN **6**, 1630001 (2016).
[29] A. Brataas, Y. V. Nazarov, and G. E. W. Bauer, Phys. Rev. Lett. **84**, 2481 (2000); Eur. Phys. J. B **22**, 99 (2001).
[30] M. Weiler, M. Althammer, M. Schreier, J. Lotze, M. Pernpeintner, S. Meyer, H. Huebl, R. Gross, A. Kamra, J. Xiao, Y.-T. Chen, H. J. Jiao, G. E. W. Bauer, and S. T. B. Goennenwein, Phys. Rev. Lett. **111**, 176601 (2013).
[31] Y. Liu, Z. Yuan, R. J. H. Wesselink, A. A. Starikov, and P. J. Kelly, Phys. Rev. Lett. **113**, 207202 (2014).
[32] A. Fert and S. F. Lee, Phys. Rev. B **53**, 6554 (1996).
[33] K. Eid, D. Portner, J. A. Borchers, R. Loloee, M. A.-H. Darwish, M. Tsoi, R. D. Slater, K. V. O'Donovan, H. Kurt, W. P. Pratt, Jr., and J. Bass, Phys. Rev. B **65**, 054424 (2002).
[34] J. Bass and W. P. Pratt, Jr., J. Phys.: Condens. Matter **19**, 183201 (2007).
[35] C. T. Boone, H. T. Nembach, J. M. Shaw, and T. J. Silva, J. Appl. Phys. **113**, 153906 (2013).
[36] K. Kondou, H. Sukegawa, S. Mitani, K. Tsukagoshi, and S. Kasai, Appl. Phys. Express **5**, 073002 (2012).
[37] W. Zhang, V. Vlaminck, J. E. Pearson, R. Divan, S. D. Bader, and A. Hoffmann, Appl. Phys. Lett. **103**, 242414 (2013).
[38] H. J. Jiao and G. E. W. Bauer, Phys. Rev. Lett. **110**, 217602 (2013).
[39] L. Bai, P. Hyde, Y. S. Gui, C. M. Hu, V. Vlaminck, J. E. Pearson, S. D. Bader, and A. Hoffmann, Phys. Rev. Lett. **111**, 217602 (2013); L. Bai, Z. Feng, P. Hyde, H. F. Ding, and C. M. Hu, Appl. Phys. Lett. **102**, 242402 (2013).
[40] L. Liu, R. A. Buhrman, and D. C. Ralph, arXiv:1111.3702.
[41] M. Obstbaum, M. Härtinger, H. G. Bauer, T. Meier, F. Swientek, C. H. Back, and G. Woltersdorf, Phys. Rev. B **89**, 060407 (2014).
[42] M. Althammer, S. Meyer, H. Nakayama, M. Schreier, S. Altmannshofer, M. Weiler, H. Huebl, S. Geprägs, M. Opel, R. Gross, D. Meier, C. Klewe, T. Kuschel, J.-M. Schmalhorst, G. Reiss, L. Shen, A. Gupta, Y.-T. Chen, G. E. W. Bauer, E. Saitoh, and S. T. B. Goennenwein, Phys. Rev. B **87**, 224401 (2013).
[43] C. Hahn, G. de Loubens, O. Klein, M. Viret, V. V. Naletov, and J. Ben Youssef, Phys. Rev. B **87**, 174417 (2013).
[44] A. Ganguly, K. Kondou, H. Sukegawa, S. Mitani, S. Kasai, Y. Niimi, Y. Otani, and A. Barman, Appl. Phys. Lett. **104**, 072405 (2014).
[45] H. Nakayama, M. Althammer, Y. T. Chen, K. Uchida, Y. Kajiwara, D. Kikuchi, T. Ohtani, S. Geprägs, M. Opel, S. Takahashi, R. Gross, G. E. W. Bauer, S. T. B. Goennenwein, and E. Saitoh, Phys. Rev. Lett. **110**, 206601 (2013).
[46] K. Ando, S. Takahashi, K. Harii, K. Sasage, J. Ieda, S. Maekawa, and E. Saitoh, Phys. Rev. Lett. **101**, 036601 (2008).
[47] V. Castel, N. Vlietstra, J. B. Youssef, and B. J. van Wees, Appl. Phys. Lett. **101**, 132414 (2012).
[48] J. C. Rojas-Sánchez, N. Reyren, P. Laczkowski, W. Savero, J. P. Attané, C. Deranlot, M. Jamet, J. M. George, L. Vila, and H. Jaffrès, Phys. Rev. Lett. **112**, 106602 (2014).
[49] A. Azevedo, L. H. Vilela-Leão, R. L. Rodríguez-Suárez, A. F. Lacerda Santos, and S. M. Rezende, Phys. Rev. B **83**, 144402 (2011).
[50] V. Vlaminck, J. E. Pearson, S. D. Bader, and A. Hoffmann, Phys. Rev. B **88**, 064414 (2013).
[51] L. Vila, T. Kimura, and Y. C. Otani, Phys. Rev. Lett. **99**, 226604 (2007).
[52] K. Ando, M. Morikawa, T. Trypiniotis, Y. Fujikawa, C. H. W. Barnes, and E. Saitoh, Appl. Phys. Lett. **96**, 082502 (2010).
[53] Y. Kajiwara, K. Harii, S. Takahashi, J. Ohe, K. Uchida, M. Mizuguchi, H. Umezawa, H. Kawai, K. Ando, and K. Takanashi, Nature (London) **464**, 262 (2010).
[54] H. L. Wang, C. H. Du, Y. Pu, R. Adur, P. C. Hammel, and F. Y. Yang, Phys. Rev. Lett. **112**, 197201 (2014).

[55] H. Nakayama, K. Ando, K. Harii, T. Yoshino, R. Takahashi, Y. Kajiwara, K. Uchida, Y. Fujikawa, and E. Saitoh, Phys. Rev. B **85**, 144408 (2012).

[56] H. Y. Hung, G. Y. Luo, Y. C. Chiu, P. Chang, W. C. Lee, J. G. Lin, S. F. Lee, M. Hong, and J. Kwo, J. Appl. Phys. **113**, 17C507 (2013).

[57] Z. Feng, J. Hu, L. Sun, B. You, D. Wu, J. Du, W. Zhang, A. Hu, Y. Yang, D. M. Tang, B. S. Zhang, and H. F. Ding, Phys. Rev. B **85**, 214423 (2012).

[58] O. Mosendz, J. E. Pearson, F. Y. Fradin, G. E. W. Bauer, S. D. Bader, and A. Hoffmann, Phys. Rev. Lett. **104**, 046601 (2010); O. Mosendz, V. Vlaminck, J. E. Pearson, F. Y. Fradin, G. E. W. Bauer, S. D. Bader, and A. Hoffmann, Phys. Rev. B **82**, 214403 (2010).

[59] Y. Niimi, D. Wei, H. Idzuchi, T. Wakamura, T. Kato, and Y. C. Otani, Phys. Rev. Lett. **110**, 016805 (2013).

[60] M. Morota, Y. Niimi, K. Ohnishi, D. H. Wei, T. Tanaka, H. Kontani, T. Kimura, and Y. Otani, Phys. Rev. B **83**, 174405 (2011).

[61] H. Kurt, R. Loloee, K. Eid, W. P. Pratt, and J. Bass, Appl. Phys. Lett. **81**, 4787 (2002).

[62] C. T. Boone, J. M. Shaw, H. T. Nembach, and T. J. Silva, J. Appl. Phys. **117**, 223910 (2015).

[63] R. J. Elliott, Phys. Rev. **96**, 266 (1954); Y. Yafet, Phys. Lett. A **98**, 287 (1983).

[64] J. Fabian and S. D. Sarma, J. Vac. Sci. Technol. B **17**, 1708 (1999).

[65] K. Roy, Phys. Rev. Appl. **8**, 011001 (2017); in *American Physical Society (APS) March 2015 Meeting, San Antonio, Texas, Session Y28.12* (APS, New York, 2015).

[66] M. I. Dyakonov and V. I. Perel, Sov. Phys. Solid State **13**, 3023 (1972).

[67] K. M. Schep, J. B. A. N. van Hoof, P. J. Kelly, G. E. W. Bauer, and J. E. Inglesfield, Phys. Rev. B **56**, 10805 (1997); G. E. W. Bauer, K. M. Schep, K. Xia, and P. J. Kelly, J. Phys. D **35**, 2410 (2002).

[68] R. Landauer, Phys. Rev. B **52**, 11225 (1995).

[69] Y. Imry and R. Landauer, Rev. Mod. Phys. **71**, S306 (1999); R. Landauer, IBM J. Res. Dev. **1**, 223 (1957); M. Buttiker, *ibid.* **32**, 317 (1988).

[70] A. Brataas, Y. Tserkovnyak, G. E. W. Bauer, and B. I. Halperin, Phys. Rev. B **66**, 060404 (2002); A. Brataas, G. E. W. Bauer, and P. J. Kelly, Phys. Rep. **427**, 157 (2006).

[71] M. Zwierzycki, Y. Tserkovnyak, P. J. Kelly, A. Brataas, and G. E. W. Bauer, Phys. Rev. B **71**, 064420 (2005).

[72] K. Ando, T. Yoshino, and E. Saitoh, Appl. Phys. Lett. **94**, 152509 (2009).

[73] L. Liu, T. Moriyama, D. C. Ralph, and R. A. Buhrman, Phys. Rev. Lett. **106**, 036601 (2011).

[74] W. Zhang, W. Han, X. Jiang, S. H. Yang, and S. S. P. Parkin, Nat. Phys. **11**, 496 (2015).

[75] Y. Wang, P. Deorani, X. Qiu, J. H. Kwon, and H. Yang, Appl. Phys. Lett. **105**, 152412 (2014).

[76] H. Y. T. Nguyen, W. P. Pratt, and J. Bass, J. Magn. Magn. Mater. **361**, 30 (2014).

[77] M. H. Nguyen, D. C. Ralph, and R. A. Buhrman, Phys. Rev. Lett. **116**, 126601 (2016).

[78] K. Ando and E. Saitoh, J. Appl. Phys. **108**, 113925 (2010).

[79] M. Jamali, A. Klemm, and J. P. Wang, Appl. Phys. Lett. **103**, 252409 (2013).

[80] K. Garello, I. M. Miron, C. O. Avci, F. Freimuth, Y. Mokrousov, S. Blügel, S. Auffret, O. Boulle, G. Gaudin, and P. Gambardella, Nat. Nanotech. **8**, 587 (2013).

[81] D. Bhowmik, L. You, and S. Salahuddin, Nat. Nanotech. **9**, 59 (2014).

[82] A. A. Kovalev, A. Brataas, and G. E. W. Bauer, Phys. Rev. B **66**, 224424 (2002).

[83] K. Chen and S. Zhang, Phys. Rev. Lett. **114**, 126602 (2015).

[84] K. D. Belashchenko, A. A. Kovalev, and M. van Schilfgaarde, Phys. Rev. Lett. **117**, 207204 (2016).

[85] E. Sagasta, Y. Omori, M. Isasa, M. Gradhand, L. E. Hueso, Y. Niimi, Y. C. Otani, and F. Casanova, Phys. Rev. B **94**, 060412(R) (2016).

[86] D. Hou, Z. Qiu, K. Harii, Y. Kajiwara, K. Uchida, Y. Fujikawa, H. Nakayama, T. Yoshino, T. An, and K. Ando, Appl. Phys. Lett. **101**, 042403 (2012).

[87] L. Wang, R. J. H. Wesselink, Y. Liu, Z. Yuan, K. Xia, and P. J. Kelly, Phys. Rev. Lett. **116**, 196602 (2016).

[88] S. Y. Huang, X. Fan, D. Qu, Y. P. Chen, W. G. Wang, J. Wu, T. Y. Chen, J. Q. Xiao, and C. L. Chien, Phys. Rev. Lett. **109**, 107204 (2012); Y. M. Lu, Y. Choi, C. M. Ortega, X. M. Cheng, J. W. Cai, S. Y. Huang, L. Sun, and C. L. Chien, *ibid.* **110**, 147207 (2013).

[89] W. L. Lim, N. Ebrahim-Zadeh, J. C. Owens, H. G. E. Hentschel, and S. Urazhdin, Appl. Phys. Lett. **102**, 162404 (2013).

[90] Y. Yang, B. Wu, K. Yao, S. Shannigrahi, B. Zong, and Y. Wu, J. Appl. Phys. **115**, 17C509 (2014).

[91] W. Zhang, M. B. Jungfleisch, W. Jiang, Y. Liu, J. E. Pearson, S. G. E. te Velthuis, A. Hoffmann, F. Freimuth, and Y. Mokrousov, Phys. Rev. B **91**, 115316 (2015).

[92] M. Caminale, A. Ghosh, S. Auffret, U. Ebels, K. Ollefs, F. Wilhelm, A. Rogalev, and W. E. Bailey, Phys. Rev. B **94**, 014414 (2016).